

A Novel Current Control Technique for Photo Voltaic Integrated Single Phase Shunt Active Power Filter

K.Rameshkumar *[‡], V.Indragandhi **, K.Palanisamy **, Ramani Kannan***

*Research Scholar, School of Electrical Engineering, VIT University, Vellore, Tamilnadu, India.

** Associate Professor, School of Electrical Engineering, VIT University, Vellore, Tamilnadu, India

*** Assistant Professor, Electrical & Electronic Engineering Department, University of Teknologi PETRONAS, Malaysia.

(rameshvel.k@gmail.com, indragandhi.v@vit.ac.in, kpalanisamy@vit.ac.in, kreee82@gmail.com)

[‡]Corresponding Author; K.Rameshkumar*, VIT University, Vellore, India

Tel: +9047155075, rameshvel.k@gmail.com

Received: 28.03.2017 Accepted:30.04.2017

Abstract- In this paper a Model Predictive Current Control (MPCC) of single phase Photo Voltaic (PV) integrated Shunt Active Power Filter (SAPF) is proposed. A PV integrated single phase Voltage Source Inverter (VSI) is used to generate a part of the real power and compensate harmonics, reactive power of a Non-Linear Load (NLL). In this paper, a DC link voltage regulation based PI control algorithm is adopted for determining the reference current at the filter side. The performance of SAPF with PV and associated control methods like switch on response and change of nonlinear load were carried out. Also, the performance of the controller has been examined with variation in irradiance, filter inductance value and variation in controller sampling time through a simulation in MATLAB software.

Keywords Single phase shunt active filter, model predictive current control, total harmonic distortion, voltage source inverter.

1. Introduction

Over the eras, shunt active power filter has become an obligatory necessity in AC power network for mitigating harmonics and reactive power compensation. This scenario is also integrated with renewable system such as photovoltaic, wind and fuel cell. Where photovoltaic being the leading power source in the renewable energy, a few concerns top up in operating it when linked with an active filter in the electric power system network such as injection of electrical energy into the grid with harmonic current and reactive power compensation. Many electrical loads draw a non-sinusoidal current from the utility supply system which is called as Non Linear Loads such as light-emitting diode lamps, variable speed drives, florescent lamps, arc furnaces, switched mode power supply and welding equipment.

These loads are mainly composed of power electronic devices, they are nonlinear in nature which gives rise to the generation of harmonics. This harmonics leads to the rise of

THD level and cause adverse effects in the power system equipment's causing overload, overheating and interference in communication networks [1-6].To overwhelm this effects in power grid, Initially passive filters was in use and it was not that much effective since it has dropdown such as fixed compensation, large size, poor performance for mitigating harmonics and resonance problem [2].

To overcome this drawback, the active filter usage came in to existence. This regular active filter is used in compensation of current harmonic and reactive power. Meanwhile PV integration to the SAPF, which produces a real power to load along with compensation of current harmonic and reactive power. This paper examines the design, analysis and implementation of Model predictive current control of single phase PV integrated SAPF. The desired output is obtained by connecting PV arrays in series and parallel and in order to extract maximum potential power from the PV array. In order to increase the voltage from PV array a boost converter is used.

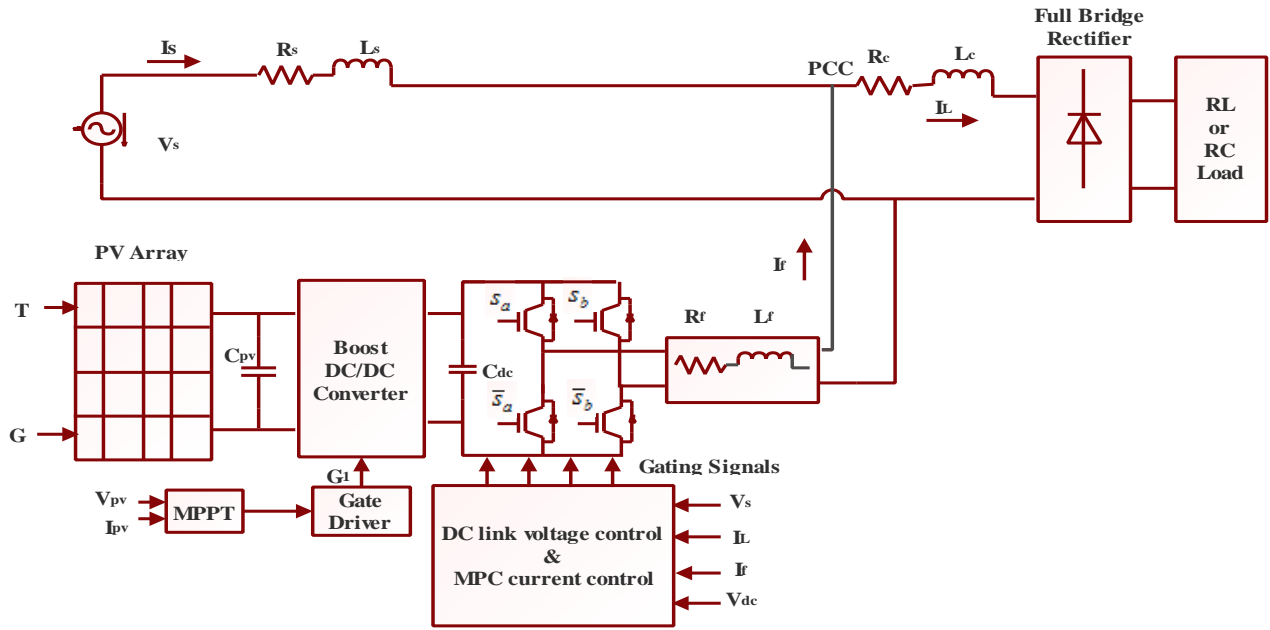


Fig. 1. Single phase PV based SAPF model.

The SAPF operation mainly depends on two factors, such as reference current extraction and current control. Many harmonic extraction theories have been proposed in literature [7-13] and these theories can be classified into (i) Frequency domain technique [2] (ii) time domain techniques. Frequency domain techniques are not preferred for real time control of SAPF when compare to time domain technique because of its slow response, high memory requirement and requiring heavy controller computation burden.

In time domain control technique researchers are mainly preferred proportional integral control algorithm [4-7], PQ strategy [8, 9] synchronous reference frame (SRF) technique [14], Artificial Neural Network (ANN) and Fuzzy Logic control (FLC) techniques [16, 17]. These extraction techniques generate the reference current for harmonic and reactive power compensation. The SRF and DQ strategies shows good performances in terms of fast response. But it has some disadvantages such as use of transformation techniques like Hilbert transform, requires high computational load for generation of fictitious phase signal, and grid frequency variation can cause an error in the reference current calculation.

The ANN and FLC technique are used for extraction of reference current. However the ANN needs training of network and FLC scheme necessitates the knowledge base to generate the rule. Thus it requires complex computation and large memory size. Hence among all the techniques most popular addressed techniques is DC link voltage regulation based PI control algorithm due to its simple implementation and less complexity. So in this proposed work a simple DC link capacitor voltage regulation based PI control algorithm is used for extracting reference current. Various current control methods have been put forward in literature for generating the gating signals to SAPF. The conventional current control techniques are used in SAPF are Pulse Width Modulation (PWM) technique [18, 19] and predictive PWM technique

[16]. However, these methods require modulation stage to generate the gate pulse to the SAPF. Hence as an alternative to PWM methods, such as hysteresis current control [2, 19], double band hysteresis control [7] method are used in literature for control of SAPF. These control techniques have the merits of absence of modulation stage and simple to implementation steps. Therefore from the literature it has been observed that there is a need of simple and accurate current tracking technique.

Henceforth in this manuscript a new model predictive current control algorithm is used for reference current tracking due to its high accuracy, simple concept and easy addition of system nonlinearities [22]. Recently many researchers show their interest towards Model Predictive Current Control (MPCC) for power converters [20-25], shunt active power filter [26, 27] and PV integrated three phase SAPF [28].

In [26-28] a simple performance indices such as total harmonic distortion (THD) is used to assess the performance of controller. Though only source current THD is not sufficient to analyse the performance of MPC controller, meanwhile the assessment reflect only the amount harmonic content in the source current. Approaches in [20, 21] consider the indices such as total harmonic distortion (THD) and switching frequency (Fsw) are used to assess the performance of controller. Here in this manuscript MPC control algorithm is used to control the PV integrated SAPF by considering all performance indices in different cases. The main contribution of this work summarizes the discrete time model of single phase SAPF system, MPC control of SAPF and various performance analysis. It includes change of nonlinear loads, switch on and off operation between PV and SAPF, irradiance changes, sampling time variation and filter inductance variation are studied by using both RL and RC Load.

The rest of the paper is organized as follows. In Section 2, integration of PV system with single phase SAPF is discussed,

In Section 3, the control strategies of SAPF with PV system are presented with clear illustration. In Section 4, simulation results are given. The paper ends with suitable conclusion drawn.

2. Integration of PV Ssystem with Single Phase Shunt Active Power Filter

In this proposed system the single phase SAPF is connected to the PV system as shown in Figure 1. It consist of PV array, DC –DC converter and single phase VSI connected to the grid at the point of PCC through a filter inductance. It consist of two types of nonlinear loads. The first nonlinear load is made by using a single-phase uncontrolled bridge rectifier with R-L load and the second nonlinear load is designed using same rectifier with R-C Load. The parameters of the PV array is shown in Table 1. A PV array output is amplified by DC-DC converter for getting the maximum power.

To obtain the maximum power from PV array various MPPT techniques were developed by researchers in [15, 29-32]. In this manuscript a simple incremental conductance MPPT technique is used for controlling the DC-DC converter switching duty cycle due to its certain advantages [30]. Then, the single phase VSI converts the DC power into AC power which is injected into the utility. In this PV based SAPF system two stage configuration is preferred because when compare to single stage two stage configuration needs lesser number of PV array, which is significantly reduces the total cost of the system.

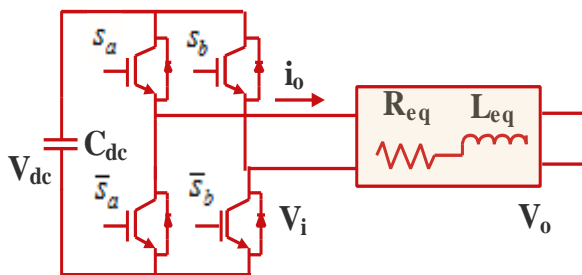


Fig. 2. Single phase VSI model

Table 1. PV array parameters (Canadian Solar CS5P-220M) at 1000W/m2 irradiance

Parameter	Values
Open circuit voltage (V _{oc})	59.26 V
Voltage at maximum power (V _{mp})	48.32 V
Short circuit current (I _{sc})	5.092 A
Current at maximum power (I _{mp})	4.547 A
Number of series (N _{ser}) and parallel (N _{par}) connected module per string	3 and 1

2.1. Single Phase Voltage Source Inverter Model

The single phase VSI model is shown in Figure 2. The output voltage of inverter, measured from negative point of DC-Link N, that can be represented in terms of switching states as follows

$$V_i = V_{dc}(S_a - S_b) \tag{1}$$

Where V_i is the inverter output voltage, V_{dc} is the DC link voltage and S_a & S_b are the control signal of inverter respectively. The mathematical model of single phase SAPF from the Figure. 2 can be expressed as

$$V_o = V_i - R_{eq}i_o - L_{eq} \frac{di_o}{dt} \tag{2}$$

Where R_{eq}, L_{eq} are the equivalent resistance and inductance of single phase SAPF system which can also be written as $R_{eq} = R_f$ and $L_{eq} = L_s + L_f$ [35].

3. Control Strategy of PV integrated SAPF

The control strategy of PV integrated SAPF is implemented over and done with two steps, such as extraction of reference compensating current and generation of gate signals for power switching devices of Voltage source inverter. The operation of PV integrated single SAPF is shown in Figure. 1. Without PV integration, the load current can be represented as

$$i_L = i_S + i_F \tag{3}$$

Where i_S - source current, i_F - filter current, which is generated by inverter based configuration, otherwise it can be represented as inverter current (i_{inv}) and i_L -load current, which consists of fundamental component (i_1) with the occurrence of all harmonic components i_H . After connecting SAPF to the Point of common coupling (PCC), a filter current i_F is generated which compensates the harmonic current produced by the loads. That can be represented as

$$i_S = i_L - i_f = (i_1 + i_H) - i_f \tag{4}$$

By connecting PV, a PV current (i_{PV}) also added with inverter current (i_{inv}). Then the load current can be represented as

$$i_L = i_S + (i_{inv} + i_{PV}) \tag{5}$$

Where $i_f = i_{inv} + i_{PV}$

After employing PV, the source current is significantly reduced from its normal value. But the load current continuously remains before as well as after compensation.

3.1. Extraction of reference compensating current

The basic principle of this extraction technique is to control capacitor voltage by using PI control algorithm is shown in Figure 3.

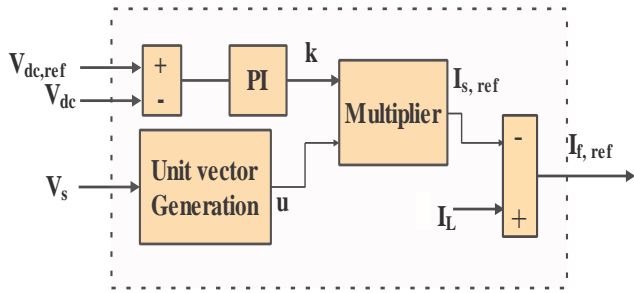


Fig. 3. Indirect PI control algorithm

Initially by comparing the voltage across the capacitor with its reference value and the output is fed to a Proportional Integral (PI) controller. The output of PI controller is taken as the peak value of reference source current ($I_{s,ref}$). Then output of PI controller is multiplied by a unit amplitude of sine wave to obtain the reference source current (I_s,ref).

$$i_{s,ref} = k * u = k * \sin \omega t \tag{6}$$

The value of k is obtained by an outer voltage loop by using PI controller as follows

$$k = k_p (V_{dc,ref} - V_{dc}) + k_i \int (V_{dc,ref} - V_{dc}) dt \tag{7}$$

Where V_{dc} the DC is link voltage, k_p and k_i are the proportional and integral gains of controller respectively. The unit sine wave u is estimated by using supply voltage (V_s) and its peak value (V_{sm}). Then the reference source current is subtracted from the load current which gives reference filter current as follows.

$$i_{f,ref} = I_L - i_{s,ref} \tag{8}$$

Finally the reference current is compared with actual filter current by using MPC control to generate gating signals for SAPF.

3.2. Model Predictive Current Control

Traditionally, SAPF have been controlled by using various current controllers. Among all control methods, MPCC technique is used in SAPF application for its effective transient state performance, because it can quickly follow the current reference signal while maintaining a constant DC-Link voltage [23]. In this paper one step prediction horizon [22] is considered in order to simplify the analysis and to reduce the computation burden. A block diagram of MPCC applied to the single phase VSI is shown in Figure. 4. A discrete time model of SAPF system is used to predict the future value inverter output current (I_f) at the instant of ($k+1$) from inverter output voltage ($V_i(k)$), inverter input voltage (V_o) and inverter output current or filter current (I_f) at the instant of k [22]. In [23] the V_o is considered as V_s .

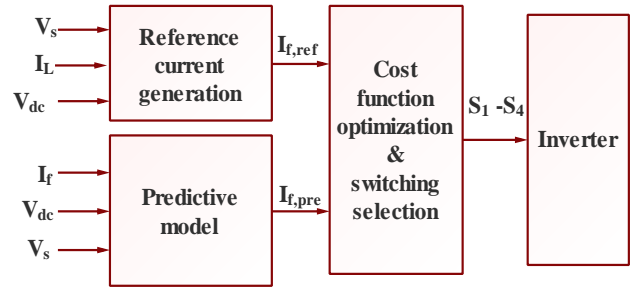


Fig. 4. Model Predictive Current Control

The first-order approximation of the derivative is considered to estimate the filter current at the instant of $k+1$ with a sampling period T_s can be written as

$$\frac{di_o}{dt} = \frac{i_f(k+1) - i_f(k)}{T_s} \tag{9}$$

Then 4 possible predicted filter current values of the single phase VSI related with the inverter output voltage V_i can be attained from (2) and (10) as

$$i_{f,pre}(k+1) = \frac{T_s}{L_{eq}} (V_i(k) - V_s(k)) + \left(1 - \frac{R_{eq} T_s}{L_{eq}}\right) i_f(k) \tag{10}$$

Where T_s is the sampling time value.

In order to apply the optimal switching signal to the VSI, the 4 predicted filter current values are compared with the reference filter current using a quality function or cost function 'g', as represented as

$$g = (i_{f,ref}(k+1) - i_{f,pre}(k+1))^2 \tag{11}$$

The MPCC method employs the optimization algorithm to attain the cost function 'g' value close to zero. During each sampling period the minimum value of 'g' is selected from 4 possible functional values. Therefore, the control algorithm choose the switching state which is going to minimize the cost function and then given to VSI directly.

3.2.1 MPCC algorithm

The MPCC algorithm is implemented in MATLAB embedded function block. The functional block operates in the discrete update technique which is based on sampling time defined for the algorithm. The parameters used in this algorithm are initialized with specific values in step 1. In step II the estimate voltage vectors and to predict the filter current at the instant of ($k+1$). The cost functions are calculated in step III. In step IV optimal cost function selection is implemented. Finally the switching state which is going to minimize the cost function is selected and given to the VSI, which is shown in step 5.

I.Parameter initialization: Set the equivalent resistance and inductance values as 0.01Ω and $5.1mH$ respectively, define the sampling frequency as 10 kHz , fixing the switching state number i to 1 and optimal cost function value to infinity. The switching states (S_i) of VSI are 0 0, 0 1, 1 0 and 1 1.

II .Prediction of voltage vector and current

For i = 1 to 4 /* four switching state*/

$$V_i = V_{dc} \begin{bmatrix} 1 & 0 \\ 0 & 1 \end{bmatrix} \cdot [S_i]^T$$

Voltage vector

by using DC link voltage and switching state ($S_1 - S_4$) */

Prediction of filter current at instant k+1

$$i_{f,pre}(k+1) = \frac{T_s}{L_{eq}} (V_i(k) - V_s(k)) + \left(1 - \frac{R_{eq}T_s}{L_{eq}} \right) i_f(k)$$

/* using filter current, inverter output voltage ($V_1 - V_4$) and supply voltage V_s */

III. Calculate the quality or cost function

$g = (i_{f,ref}(k+1) - i_{f,pre}(k+1))^2$ /*by using reference and actual filter current */

IV. Selection of optimal Cost function

If ($g < g_{opt}$)

$g_{opt} = g$ /*updating optimal cost function*/

$X_{opt} = I$ /*updating optimal switching state*/

End

End

V. Optimum switching state.

$S_a = S(x_{opt}, 1), S_b = S(x_{opt}, 2)$ /* optimal switching state is given to inverter*/

The obtained optimal switching signal is given to VSI and this algorithm continuing by restart with step 1. Based on the switching signal, the I_f and V_{dc} changes and I_s also changes.

Table 2. Single phase SAPF Parameters.

Parameters	Value
Supply voltage (V_s)	230 V
Supply frequency (f)	50 Hz
DC link voltage (V_{dc})	400 V
DC link capacitance (C_{dc})	4700 μ F
Source resistance (R_s) & Inductance (L_s)	0.1 Ω & 1 mH
Series load resistance(R_c) & inductance (L_c)	0.01 Ω & 1 mH
Filter resistance (R_f) & Inductance (L_f)	0.01 Ω & 5 mH
Sampling time (T_s)	10 μ s
PV module capacitance (C_{PV}) & Inductance (L)	2200 μ F & 400 μ H
RL load and RC load	15 Ω ,160 mH & 20 Ω & 100 μ F

4. Simulation Results

The MATLAB Simulink model of PV integrated SAPF is developed and executed to compensate the reactive power and harmonic compensation, where a single phase non-linear load are fed the power from both utility supply and PV system . The parameters of system is shown in Table 2. The performance analysis of MPC based SAPF has been analysed with five different cases as follows: Switch on response, transient response, solar irradiance variation, filter inductance variation and varying the sampling time. The value of total harmonic distortion (THD) and average device switching

frequency (fsw) are calculated according to the guidelines given in [20, 25].

4.1. Switch on response (RL load and RC load) - Case 1

The MPCC of SAPF dynamic performance is examined by two modes. In first mode switched on the SAPF at 0.1 s, it operate as full SAPF operation (FSAPF) mode to compensate the harmonic current and reactive power of the loads. In second case PV is switched on at 0.52 s, this condition is called as partial real power injection with SAPF (PRPI with SAPF) mode. In this mode SAPF compensate the current harmonics and reactive power and also inject a part of real power required by the. Before connecting the SAPF to the PCC, from 0 to 0.1s, the source current waveform is exactly similar to the load current. When the THD for the source current is 38.5% and 46.2% for RL and RC non-linear load respectively.

During that time the RL and RC loads draw real and reactive powers only from utility main. When SAPF is on, it injects reactive power and compensating current to the PCC, which is required for the load and makes the source reactive power to be zero and source current harmonics becomes within the limit of IEEE 519-1992 standard. It can be noticeable how the source current becomes pure sinusoidal and in phase with voltage since the SAPF entirely compensates the harmonics and reactive power of the nonlinear loads. But the nonlinear loads still draws active power from the utility mains.

A part of real power to the load is also injected at PCC when the PV is turned on. Hence forth source real power is reduced as shown in Table 3. As impact of this action the source current magnitude also significantly reduced. The source voltage (V_s), source current (I_s), load current (I_L), filter current (I_f) and DC link voltage (V_{dc}) are shown in Figure 5 and 7. The real and reactive power of three parts, contains the source, load and filter is illustrated in Figure 6 and 8 for both load conditions.

4.2. Transient Response - (Case 2)

The SAPF system transient performance has been evaluated by two scenarios. In first scenario the load changes from RL-load to RC-load at 0.5 s without PV integration and the load changes from RC to RL load at 0.52 s with PV integration in second scenario. The source voltage (V_s), source current (I_s), load current (I_L), filter current (I_f) and DC link voltage (V_{dc}) for both scenarios are depicted in Figure 9 and 10. It is resulted from these figures a good tracking of their references and fast transient response of the SAPF with a settling time of about nearly 150 ms is achieved.

4.3. Solar irradiance Variation - (Case 3)

In this case the current reference tracking behaviour is analysed with variable irradiance conditions with RL and RC load condition. Figure 11 and 12 illustrates the inverter switching frequency and source current RMS value under different solar irradiance (0 W/m², 100 W/m², 200 W/m², 300 W/m², 500 W/m², 600 W/m², 800 W/m², and 1000 W/m²) conditions.

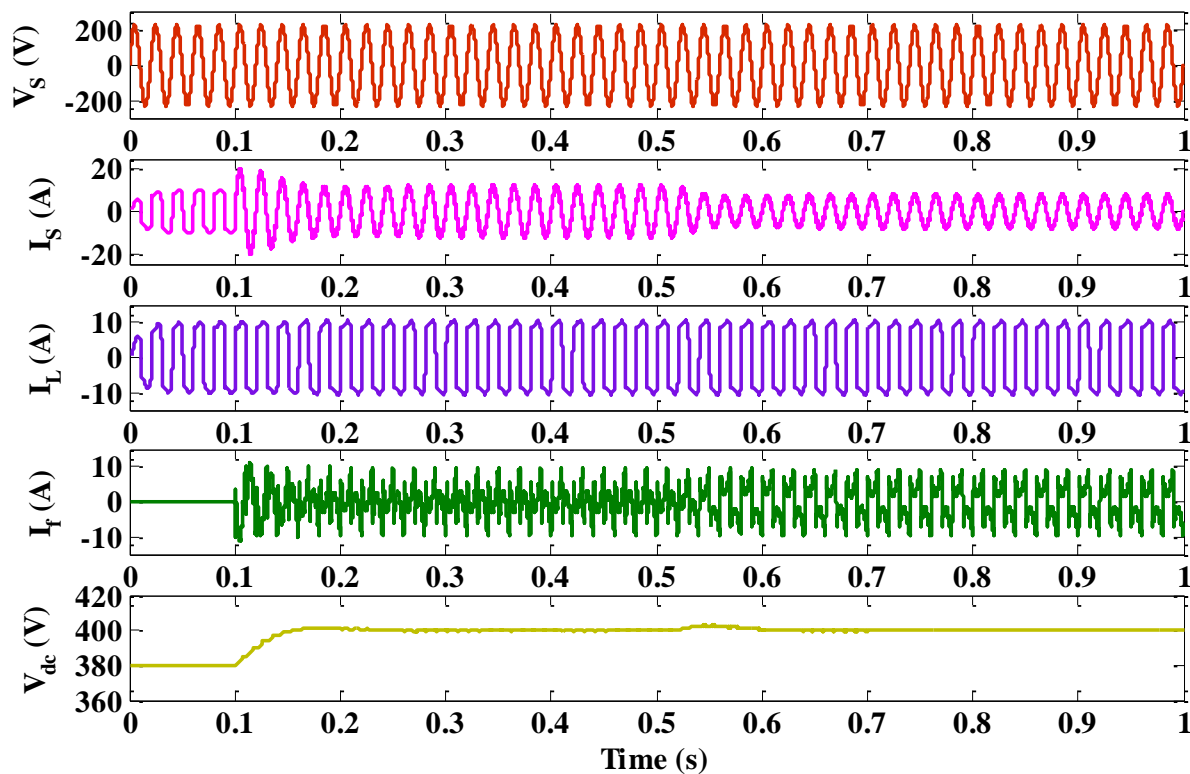


Fig. 5. V_s , I_s , I_L , I_f and V_{dc} for RL load switch on response

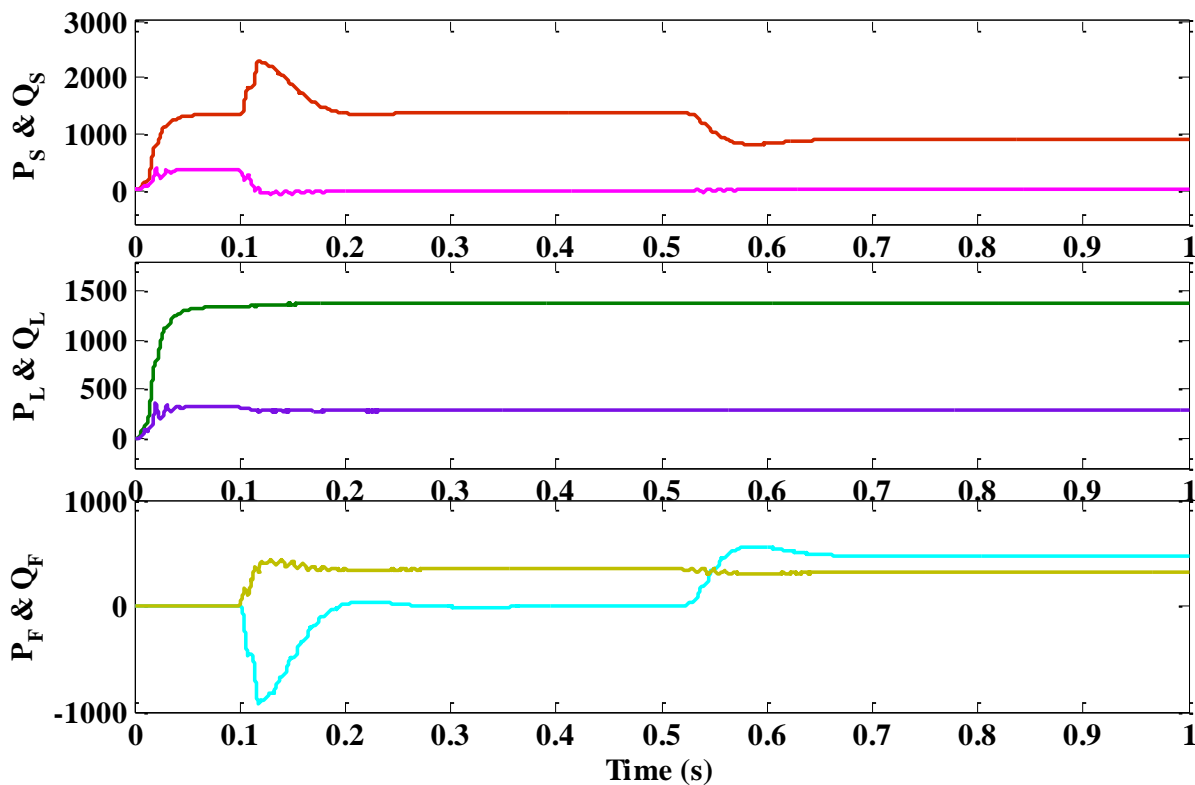


Fig. 6. P_s & Q_s , P_L & Q_L and P_F & Q_F for RL load ($P_{s,L,F}$ (W) & $Q_{s,L,F}$ (Var))

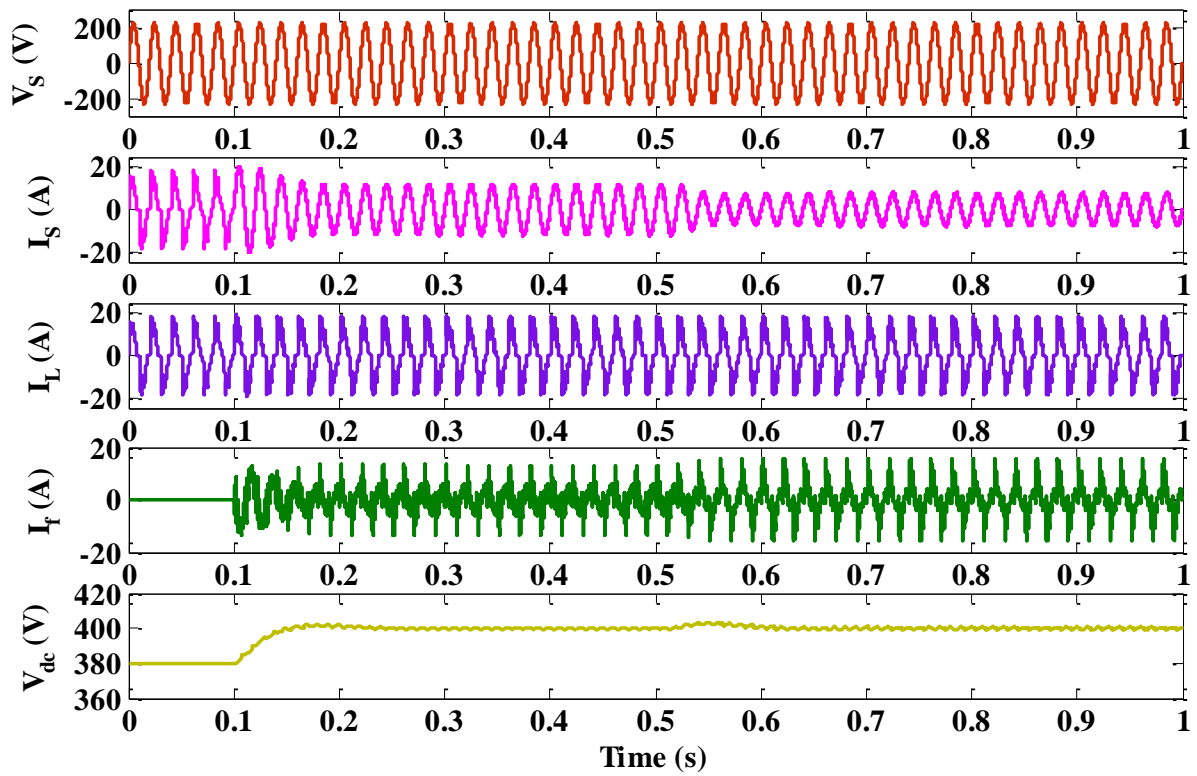


Fig. 7. V_s , I_s , I_L , I_f and V_{dc} for RC load switch on response

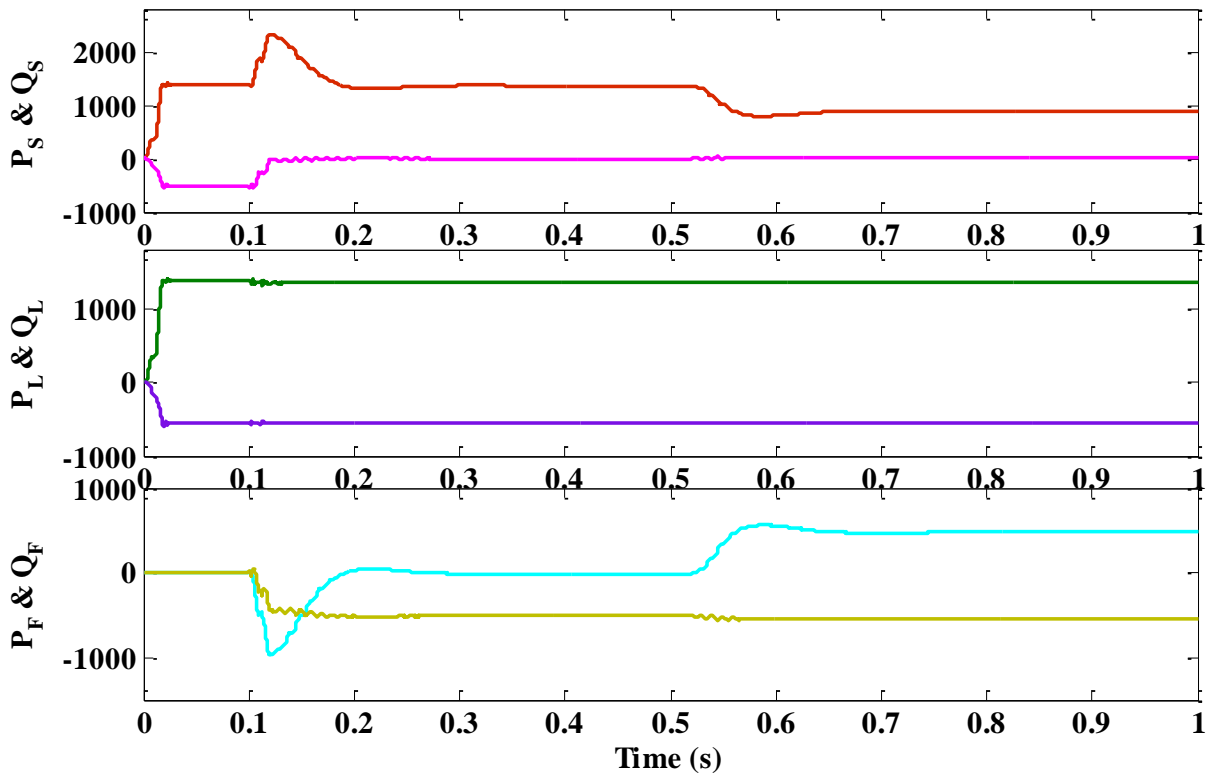


Fig. 8. P_s & Q_s , P_L & Q_L and P_f & Q_f for RC load switch on response ($P_{s,L,F}$ (W) & $Q_{s,L,F}$ (Var))

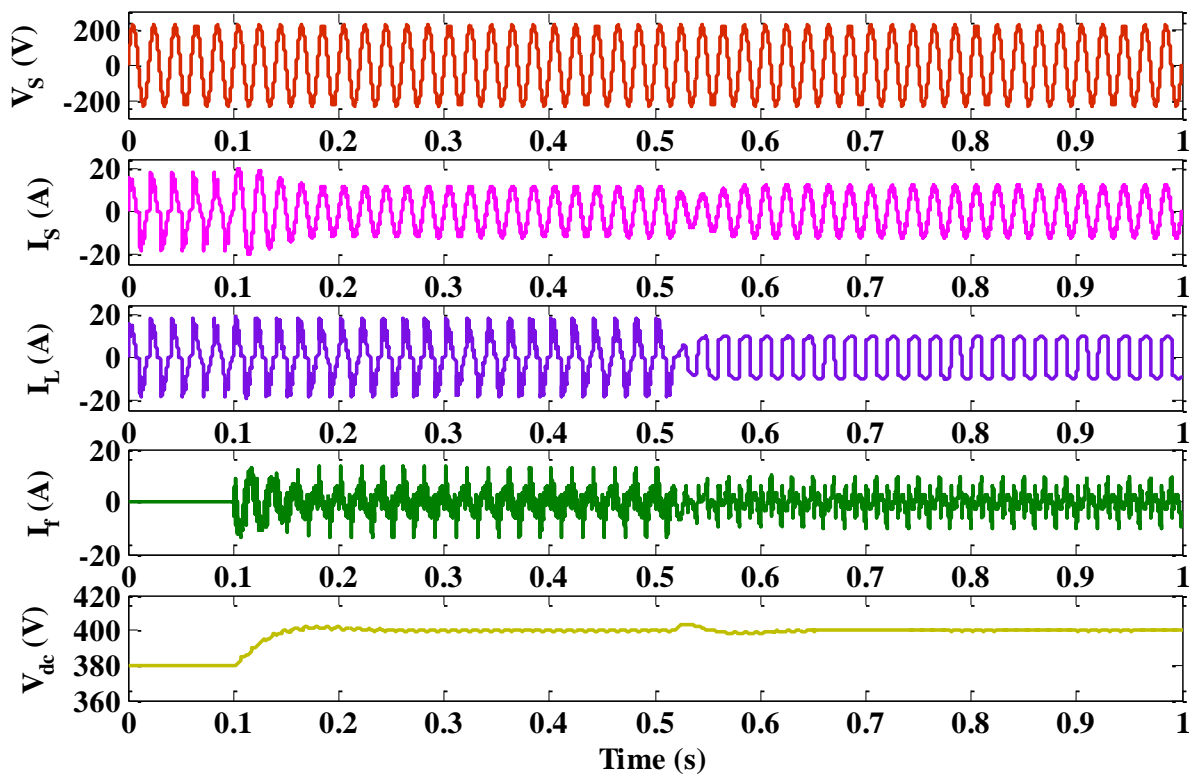


Fig. 9. V_s , I_s , I_L , I_f and V_{dc} for RC-RL transient response-Without PV (FSAPF Mode)

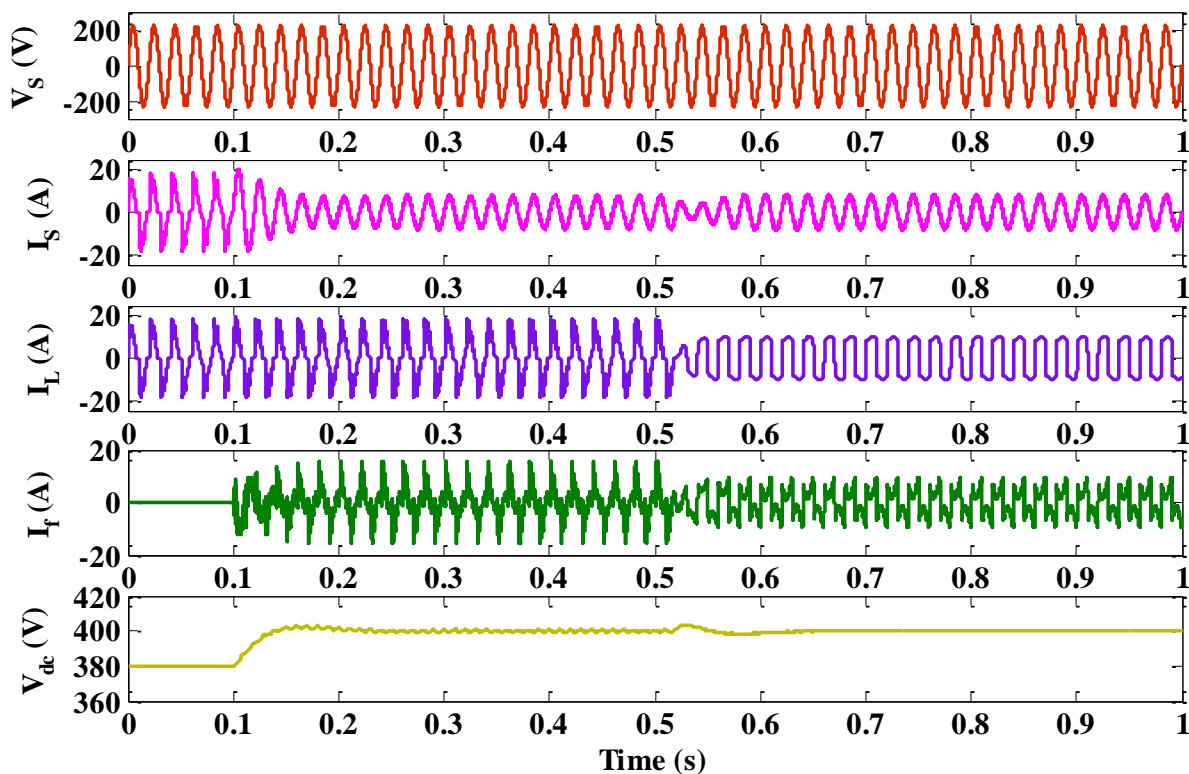


Fig 10. V_s , I_s , I_L , I_f and V_{dc} for RC-RL transient response-With PV (PRPI with FSAPF Mode)

Firstly, the PV SAPF is switched on until the DC link voltage reaches its set value. Once the DC link voltage reach their set value, to change the solar irradiance.

Fig 12. Switching frequency F_{sw} and THD, RMS value of Source current (I_s) of RC load for varying irradiance conditions. From the Figure 11 and 12 illustrate that the variation of F_{sw} and THD from zero to high value of irradiances. By increasing the irradiance which directly reduces the source current and increases the SAPF current. The source current reduction due to PV, which automatically increase the small amount of THD values. The switching frequency is almost constant for all value of radiations.

4.4. Performance of MPC controller for filter inductance variation - (Case 4)

The accuracy of proposed controller mainly depends upon the discrete model of the system and parameters value. The filter inductor variation have been examined through the simulation for both RL and RC load with and without PV integration. In this case the sampling time of T_s is $10\mu s$ considered and the filter inductance value (L_f) are taken to changes from 0.5 mH to 15 mH. In this analysis, two cases are considered: First case (CFI)-Changes to the filter inductance and no change in controller, where the controller is unaware about L_f changes and it run at a rated L_f value (5mH).

In second case (CFIC) - Changes to the filter inductance and controller where the controller knows the L_f variations. In this analysis the comparison have been done in in terms of THD and switching frequency, and that are presented in Table 4 and 5.

Even though the filter parameter changes the controller to select the switching state which give minimum error in the reference current tracking.

From the Table 4 and 5, it can be observed that the difference between CFI and CFIC cases it's found that the values are small in L_f range lying between 5mH - 10mH. The minimum value of L_f to increase the source current THD and inverter switching frequency in both with PV and without PV states.

Table 3. P_s & Q_s , P_L & Q_L and P_F & Q_F during switch on response condition

PV-SAPF	SAPF off state	SAPF on state					
		FSAPF		PRPI +SAPF			
Source power (W)							
		P_s	Q_s	P_s	Q_s	P_s	Q_s
Load	RL	1400	380	1400	0	750	0
	RC	1380	-560	1380	0	740	0
Load power (W)							
		P_L	Q_L	P_L	Q_L	P_L	Q_L
Load	RL	1400	380	1400	380	1400	380
	RC	1380	-560	1380	-560	1380	-560
Filter power (W)							
		P_F	Q_F	P_F	Q_F	P_F	Q_F
Load	RL	0	0	0	380	650	380
	RC	0	0	0	-560	640	-560

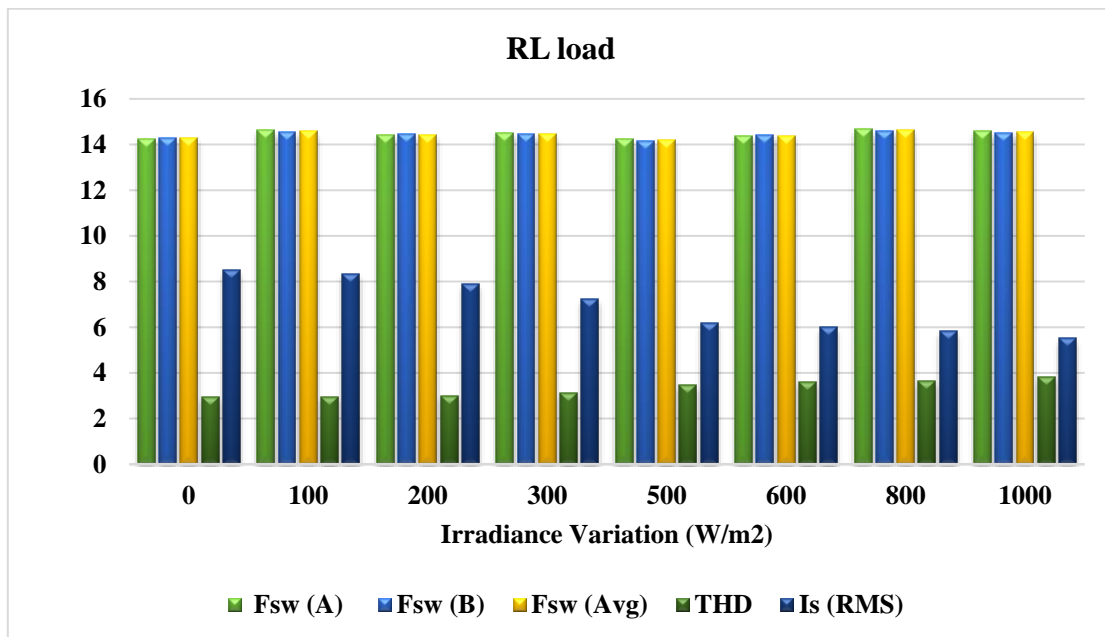


Fig. 11. Switching frequency F_{sw} and THD, RMS value of Source current (I_s) of RL load for varying irradiance conditions

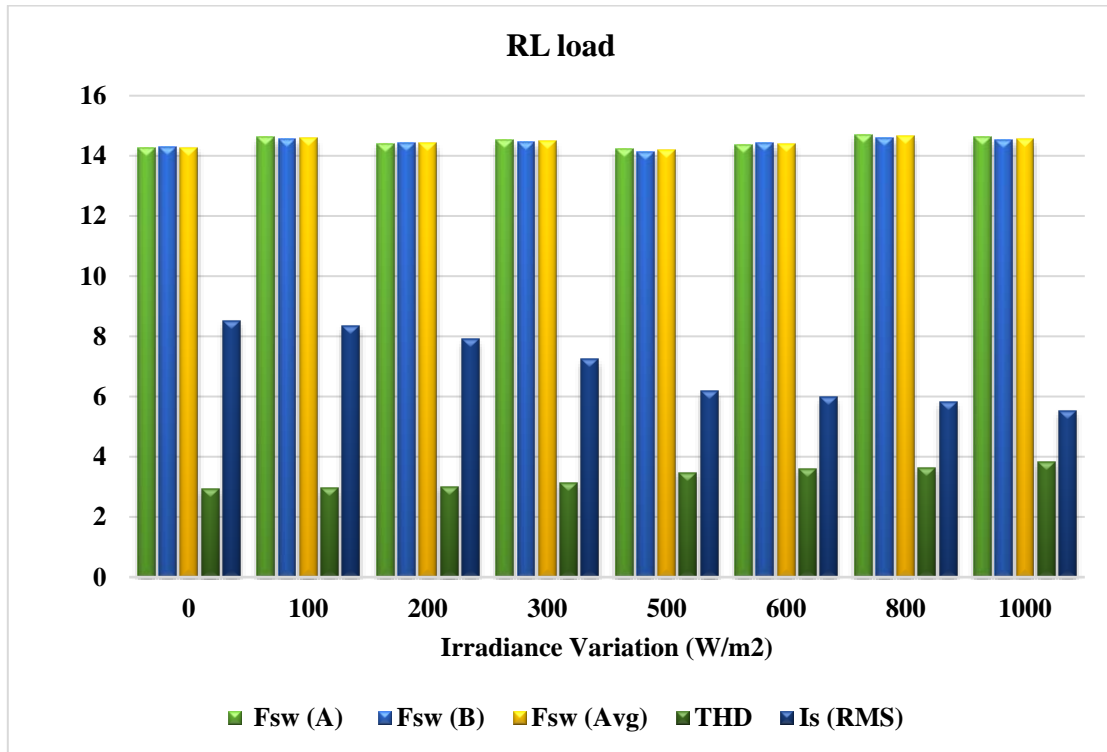


Fig. 12. Switching frequency F_{sw} and THD, RMS value of Source current (I_s) of RC load for varying irradiance conditions

Table 4. Comparison of THD and F_{sw} with filter parameter variation for RL and RC loads not considering PV

Load	Lf Value	Without PV							
		THD	CFI			THD	CFIC		
			F_{sw} (kHz)				F_{sw} (kHz)		
			Leg A	Leg B	Avg		Leg A	Leg B	Avg
RL Load	0.5mH	9.98	24.350	23.245	23.797	16.772	14.225	13.970	14.097
	1mH	6.96	20.780	19.670	20.225	8.77	14.265	14.285	14.275
	3mH	3.48	14.630	14.665	14.648	3.98	14.485	14.365	14.425
	5mH	2.94	14.305	14.320	14.313	2.94	14.305	14.305	14.305
	7mH	2.90	14.385	14.175	14.280	2.55	14.345	14.405	14.375
	10mH	2.97	13.995	14.180	14.087	2.37	14.430	14.550	14.490
	12mH	3.37	13.680	13.710	13.695	2.60	14.185	13.725	13.955
	15mH	4.86	13.585	13.795	13.690	3.68	13.895	13.965	13.930
RC Load	0.5mH	7.85	21.650	21.995	21.822	14.26	13.930	14.005	13.967
	1mH	5.04	17.765	16.640	17.202	6.25	14.200	14.075	14.137
	3mH	2.79	14.420	14.700	14.560	2.57	14.060	14.230	14.145
	5mH	2.22	13.895	14.125	14.010	2.22	13.895	14.125	14.010
	7mH	2.14	13.745	13.455	13.600	2.31	13.985	13.095	13.540
	10mH	2.94	11.845	11.795	11.820	2.50	12.620	12.845	12.732
	12mH	3.11	10.785	11.025	10.905	2.47	11.735	11.790	11.762
	15mH	3.58	8.595	8.740	8.6675	2.38	11.470	10.925	11.197

Table 5. Comparison of THD and F_{sw} with filter parameter variation for RL and RC loads Considering PV

Load	Lf Value	With PV							
		CFI				CFIC			
		THD	F_{sw} (kHz)			THD	F_{sw} (kHz)		
			Leg A	Leg B	Avg		Leg A	Leg B	Avg
RL Load	0.5mH	15.38	24.175	24.100	24.137	24.65	14.075	14.125	14.100
	1mH	10.30	20.425	20.725	20.575	13.77	13.915	13.770	13.842
	3mH	4.80	14.680	14.815	14.747	5.67	14.320	14.495	14.407
	5mH	3.82	14.615	14.530	14.572	3.82	14.615	14.530	14.572
	7mH	3.64	14.325	14.245	14.285	3.05	14.585	14.325	14.455
	10mH	4.06	14.200	13.880	14.040	3.83	14.040	14.065	14.052
	12mH	5.22	13.980	13.760	13.870	3.78	14.335	13.965	14.150
	15mH	8.14	13.800	13.885	13.842	6.23	14.035	14.080	14.057
RC Load	0.5mH	12.69	22.450	22.070	22.260	21.59	13.740	13.770	13.755
	1mH	8.34	16.730	17.160	16.945	9.89	13.960	13.815	13.887
	3mH	5.07	14.750	14.555	14.652	4.45	14.315	14.255	14.285
	5mH	4.22	13.780	14.160	13.970	4.22	13.780	14.160	13.970
	7mH	3.75	13.460	13.630	13.545	4.13	13.285	13.675	13.480
	10mH	4.77	12.065	11.770	11.917	4.43	12.855	12.365	12.610
	12mH	4.98	10.615	10.735	10.675	4.43	11.660	11.730	11.695
	15mH	6.84	7.985	8.060	8.022	4.50	10.555	10.505	10.530

4.5. Changing the Sampling Time – (Case 5)

In order to validate the ability of the proposed MPC controller to operate with different sampling times, and effect of sampling time variation on THD and F_{sw} are shown in Figure 13 to 15. By increasing the sampling time the THD

value gradually increasing for RL and RC load conditions for both with PV and without PV states. Figure 15 shows that the PV integrated SAPF source current for both loads increases slightly for THD value due to reduction of magnitude of source current values for all sampling time. At the same time switching frequency decreases on increasing sampling time.

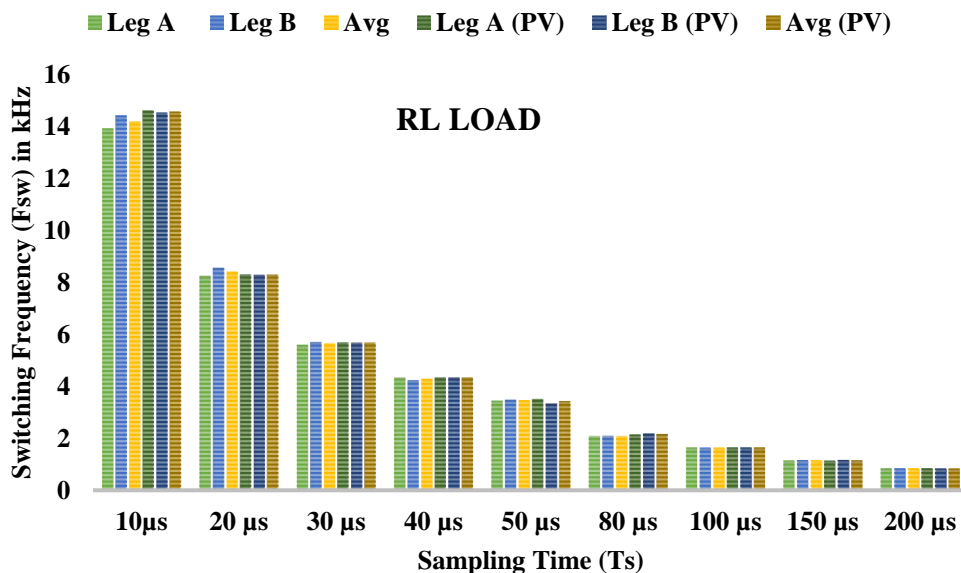


Fig 13. Switching frequency (F_{sw}) of Leg A, B and average value of Leg A & B with and without PV in RL load for varying sampling time condition

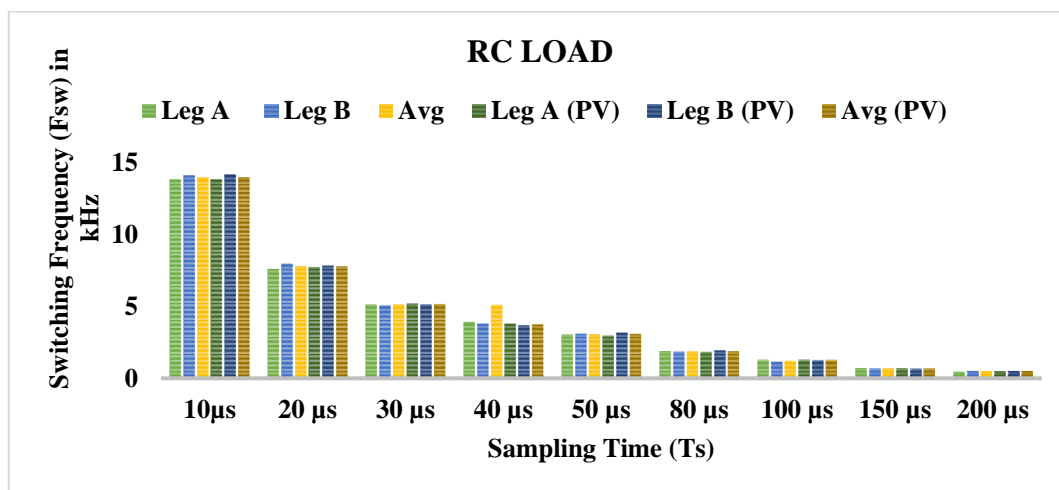


Fig. 14. Switching frequency (F_{sw}) of Leg A, B and average value of Leg A & B with and without PV in RC load for varying sampling time condition

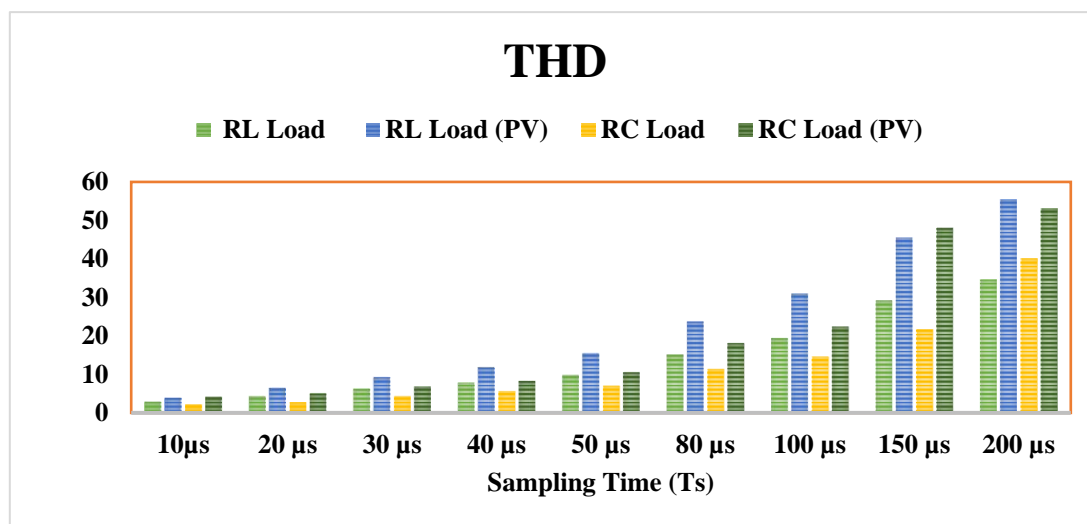


Fig. 15. THD of Source current (I_s) with and without PV in RL and RC load for varying sampling time conditions

So from the above simulated results proves that the proposed MPC control of PV integrated SAPF perform following actions: Compensation of current harmonics, reactive power compensation, SAPF with PV inject a part of real power to the load and source current THD is reduced less than 5%.

5. Conclusion

A MPCC applied to the single phase PV integrated SAPF is presented and analysed in this manuscript. The main advantage of this scheme is easy to design and implement. In this proposed method a DC link voltage regulation based PI control algorithm is employed for reference current extraction. This SAPF with PV inject a part of real power to the load and also to compensate the nonlinear load harmonics and reactive power. The technique is proved that it can be suitable for single phase SAPF with PV integration application. From the results that the MPCC control technique having good current tracking ability in both switch on, transient responses and it

can compensate the filter inductance and sampling time variations. It is alternative to classical linear control methods. Finally as the further research will focus on the simulation results will compare with the experimental results and designing the controller, in case of distorted supply condition.

References

- [1] REN21, Renewables 2015 global status report, Tech. rep., REN21 Secretariat, Paris, 2015.(Report)
- [2] R.Gupta . “Generalized frequency domain formulation of the switching frequency for hysteresis current controlled VSI used for load compensation”, IEEE Transactions on Power Electronics, Vol 27, pp.2526-35, May 2012. (Article)
- [3] Zainuri, Muhammad Ammirul Atiqi Mohd, et al. "Improved ADALINE Harmonics Extraction Algorithm for Boosting Performance of Photovoltaic Shunt Active Power Filter under Dynamic Operations." system vol. 4,pp 1-4, November 2016. (Article).

- [4] B.Singh, A.Chandra, K.Al-Haddad. "An improved single phase active power filter with optimum dc capacitor", Proceedings of the 1996 IEEE IECon 22nd International Conference , Vol. 2, pp. 677-682, 5 August 1996.(Conference paper)
- [5] P.Kumar, A.Mahajan. "Soft computing techniques for the control of an active power filter", IEEE transactions on power delivery". Vol 24, pp. 452-61, January 2009.(Article)
- [6] R.Mahanty. "Indirect current controlled shunt active power filter for power quality improvement", International Journal of Electrical Power & Energy Systems, vol 62, pp.441-449, November 2014. (Article)
- [7] H.Komurcugil. "Double-band hysteresis current-controlled single-phase shunt active filter for switching frequency mitigation. 'International Journal of Electrical Power & Energy System, vol 69, pp 131-140, July, 2015. (Article)
- [8] V.Khadkikar, A.Chandra, BN.Singh. "Generalised single-phase pq theory for active power filtering: simulation and DSP-based experimental investigation", IET Power Electronics, vol 2, pp 67-78, January 2009. (Article)
- [9] AH.Ukande, SL.Tiwari, SG.Kadwane, A.Kadu. "Generalise PQ theory with SPWM for single phase shunt active filter applications", In Power, Communication and Information Technology Conference (PCITC) IEEE, pp 89-94, October 2015. (Conference paper)
- [10] O.Aissa, S.Moulaoum, I.Colak, B. Babes, and N.Kabache, "Analysis, design and real-time implementation of shunt active power filter for power quality improvement based on predictive direct power control", International Conference on Renewable Energy Research and Applications (ICRERA), pp. 79-84, 20-23November.2016. (Conference Paper)
- [11] B. Yahia, D.Hind and C.Rachid, "The Application of an Active Power Filter on a Photovoltaic Power Generation System", International Journal of Renewable Energy Research, vol.2, no.4, pp.583-590,2012. (Article)
- [12] A. A. Elgammal, D. Ali, "Self-Regulating Active Power Filter Compensation Scheme for Hybrid Photovoltaic-Fuel Cell Renewable Energy System for Smart Grid Applications", International Journal of Renewable Energy Research, vol.7, no.2, pp.513-524, 2017. (Article)
- [13] I.Abouddrar, S.E. Hani, H.Mediouni,N.Bennis and A. Echchaachouai, "Hybrid Algorithm and Active Filtering Dedicated to the Optimization and the Improvement of Photovoltaic System Connected to Grid Energy Quality", International Journal of Renewable Energy Research, vol.7, no.2, pp. 895-900, 2017. (Article)
- [14] Acuna P, Morán L, Rivera M, Aguilera R, Burgos R, Agelidis VG. "A single-objective predictive control method for a multivariable single-phase three-level NPC converter-based active power filter", IEEE Transactions on Industrial Electronics2, vol 62, pp 4598-607, July 2015. (Article)
- [15] FM.De Oliveira, SA. Da Silva, FR.Durand, LP. Sampaio, VD.Bacon, LB.Campanhol. "Grid-tied photovoltaic system based on PSO MPPT technique with active power line conditioning" IET Power Electronics, vol 9, pp 1180-1191, May 2016. (Article)
- [16] YM. Chen, RM. O'Connell. "Active power line conditioner with a neural network control" IEEE Transactions on Industry Applications, vol 33,pp 1131-1136, July 1997. (Article)
- [17] LH.Tey, PL.So, YC.Chu. "Improvement of power quality using adaptive shunt active filter" IEEE transactions on power delivery, vol 20, pp 1558-15568, April 2005. (Article)
- [18] JC.Wu, HL.Jou. "Simplified control method for the single-phase active power filter". IEE Proceedings-Electric Power Applications, vol 143, pp 219-224, May 1996. (Article)
- [19] P.Anjana, V.Gupta, H.Tiwari, N.Gupta, R.Bansal. "Hardware Implementation of Shunt APF Using Modified Fuzzy Control Algorithm with STM32F407VGT Microcontroller". Electric Power Components and Systems, vol 44, pp 1530-1542, August 2016. (Article)
- [20] MS.Hamad, AM. Fahmy, M.Abel-Geliel. "Power quality improvement of a single-phase grid-connected PV system with fuzzy MPPT controller". Industrial Electronics Society, IECON 2013-39th Annual Conference of the IEEE, pp 1839-1844, November 2010. (Conference paper)
- [21] J.Rodriguez, J.Pontt, CA.Silva, P.Correa, P.Lezana, P.Cortés, U.Ammann. "Predictive current control of a voltage source inverter". IEEE Transactions on Industrial Electronics. Vol 54, pp 495-503, February 2007. (Article)
- [22] S.Kouro , P. Cortés, R.Vargas,U. Ammann, J.Rodriguez. "Model predictive control—A simple and powerful method to control power converters". IEEE Transactions on Industrial Electronics. Vol 56, pp 1826-1838, June 2009. (Article)
- [23] J.Rodriguez, MP. Kazmierkowski, JR.Espinoza, P. Zanchetta , H.Abu-Rub, HA Young,CA.Rojas. "State of the art of finite control set model predictive control in power electronics". IEEE Transactions on Industrial Informatics. Vol 9, pp 1003-1016, May 2013. (Article)
- [24] V.Yaramasu, M. Rivera, B. Wu, J. Rodriguez. "Model predictive current control of two-level four-leg inverters—Part I: Concept, algorithm, and simulation analysis". IEEE Transactions on Power Electronics. Vol 28, pp 3459-3468, July 2013. (Article)
- [25] M.Rivera, V.Yaramasu, J.Rodriguez, B. Wu B. "Model predictive current control of two-level four-leg inverters—Part II: Experimental implementation and

- validation". IEEE Transactions on Power Electronics. Vol 28, pp 3469-3478, July 2013. (Article)
- [26] P.Acuna, L. Morán, M. Rivera, R.Aguilera, R.Burgos, VG. Agelidis. "A single-objective predictive control method for a multivariable single-phase three-level NPC converter-based active power filter". IEEE Transactions on Industrial Electronics. vol 62, pp 4568-607, July 2015. (Article)
- [27] P.Acuna, L.Morán, M. Rivera, J.Dixon, J.Rodriguez. "Improved active power filter performance for renewable power generation systems". IEEE transactions on power electronics. vol 29, pp 687-6894, February 2014. (Article)
- [28] B.Boukezata, JP.Gaubert, A.Chaoui, M.Hachemi. "Predictive current control in multifunctional grid connected inverter interfaced by PV system". Solar Energy. Pp 130-141, December 2016. (Article).
- [29] Y.Soufi, M.Bechouat, S.Kahla, and K. Bouallegue "Maximum power point tracking using fuzzy logic control for photovoltaic system", International Conference on Renewable Energy Research and Application (ICRERA), pp. 902-906 ,19-22 October. 2014. (Conference Paper)
- [30] P.Sivakumar, A. Kader, Y.Kaliavaradhan, and M. Arutchelvi, "Analysis and enhancement of PV efficiency with incremental conductance MPPT technique under non-linear loading conditions", Renewable Energy, vol 81, pp.543-550 September 2015. (Article).
- [31] A.W.Leedy, and K.E.Garcia, "An indirect method for maximum power point tracking for photovoltaic arrays", International Conference on Renewable Energy Research and Application (ICRERA), pp. 174-179, 19-22 October. 2014. (Conference Paper)
- [32] A.Cordeiro, D. Foito and V.F.Pires, "A PV panel simulator based on a two quadrant DC/DC power converter with a sliding mode controller", International Conference on Renewable Energy Research and Applications (ICRERA), pp. 928-932, 22-25 November.2015. (Conference Paper).